ELSEVIER

Journal of Structural Geology 29 (2007) 1798–1810

JOURNAL OF STRUCTURAL GEOLOGY

www.elsevier.com/locate/jsg

Paleostress analysis of heterogeneous fault-slip data: The Gauss method

Jure Žalohar*, Marko Vrabec

University of Ljubjana, Faculty of Natural Sciences and Engineering, Department of Geology, Aškerčeva 12, SI-1000 Ljubljana, Slovenia

Received 17 December 2006; received in revised form 27 June 2007; accepted 28 June 2007
Available online 20 July 2007

Abstract

We describe the *Gauss method* for reconstructing paleostress tensors from heterogeneous fault-slip data. We define *compatibility measure* and *compatibility function,* which verify the compatibility of a given stress tensor with observed fault-slip data. In order to constrain inversion results to mechanically acceptable solutions, we additionally consider the ratio between the normal and shear stress on the fault plane, since it is assumed that the results of paleostress inversion should be in agreement with the Amonton's Law. The optimal solution for stress tensors that activated the observed faults is found by searching for the global and highest local maxima of the *object function F* defined as a sum of compatibility functions for all fault-slip data. We verify the reliability of the method both by mathematical means and by numerical tests, and analyse its effectiveness in the case of large dispersion of angular misfit between the direction of slip and shear stress along the faults.

Keywords: Stress inversion; Heterogeneous fault-slip data; Fault analysis; Stress tensor separation

1. Introduction

The main goal of the paleostress analysis is to find the stress tensor, capable of explaining the direction of slip on most of the faults observed in the studied rock mass. Generally this problem is referred to by structural geologists as *the inverse problem* (Fleischman and Nemcok, 1991; Angelier, 1994; Twiss and Unruh, 1998) and can be solved using inversion algorithms published by, for example, Carey and Brunier (1974), Angelier (1979, 1984, 1989, 1994), Armijo et al. (1982), Etchecopar et al. (1981), Huang (1988), Hardcastle (1989), Will and Powell (1991), Nemcok and Lisle (1995), Nemcok et al. (1999), Arlegui-Crespo and Simón-Gómez (1998), Fry (1992, 1999, 2001), Yamaji (2000a,b), Shan et al. (2003), Orife and Lisle (2003), Liesa and Lisle (2004), Shan et al. (2006), Orife and Lisle (2006), Sato and Yamaji (2006), Otsubo et al. (2006), to name some of them. The methods of paleostress analysis proposed by these authors, while different in approach, are all based on similar basic assumptions (Nemcok and Lisle, 1995; Twiss and Unruh, 1998): (1) the direction of movement on the faults parallels the shear stress on those faults; (2) the faults do not interact (the movement along one fault is independent of the movement on the other faults); (3) the blocks bounded by the fault planes do not rotate; and (4) the stress field activating the faults is time-independent and homogeneous. From these assumptions follows the basic hypothesis of paleostress analysis: *the direction of slip on a set of differently oriented faults can be explained by a single stress tensor*. Many doubts about the validity of such assumptions appeared in the geological literature, and were discussed in detail, for example, by Dupin et al. (1993), Pollard et al. (1993), Twiss and Unruh (1998), Watterson (1999), Tikoff and Wojtal (1999), Marrett and Peacock (1999) and Pollard (2000).

The paleostress inversion problem can be most easily formulated mathematically for *homogeneous* fault systems, where all faults have been active at the same time and in the

* Corresponding author.
E-mail addresses: jure.zalohar@guest.arnes.si (J. Žalohar), marko.vrabec@ntf.uni-lj.si (M. Vrabec).

0191-8141/$ - see front matter © 2007 Elsevier Ltd. All rights reserved.
doi:10.1016/j.jsg.2007.06.009

same stress regime (e.g., Angelier, 1979, 1989, 1994; Nemcok and Lisle, 1995; Nemcok et al., 1999). Unfortunately, fault systems are seldom homogeneous. More often they have been influenced by several different stress regimes corresponding to different tectonic events (Angelier, 1989; Nemcok and Lisle, 1995). In this case the fault systems are referred to as being *heterogeneous* and composed of *homogeneous subsystems* (Angelier, 1989; Nemcok and Lisle, 1995; Nemcok et al., 1999). Several methods for analysis of such fault-slip data have been described in the literature and can be roughly grouped into three main groups: (1) methods based on the traditional stress inversion approach, which involves the concept of best-fit stress tensor; (2) methods based on the cluster analysis; and (3) methods based on Fry's (1999) sigma space concept.

The traditional stress inversion approach, which looks for the best-fit stress tensor by minimizing or maximizing some object function (whether explicitly or implicitly), was proposed by Carey and Brunier (1974), Angelier (1979, 1984), Etchecopar et al. (1981), Armijo et al. (1982), Galindo-Zaldivar and González-Lodeiro (1988), Michael (1984), and Hardcastle and Hills (1991). In these methods, the success with which a given stress tensor accounts for the recorded slip direction indicators, is usually quantified as the sum of some measure of deviation between the observed striations and those predicted from the stress tensor being considered (Nemcok and Lisle, 1995). While this approach is very suitable for analyzing homogeneous fault systems, it may be highly problematic when dealing with dynamically-heterogeneous data sets, because in such a case the object function can have multiple peaks (Yamaji et al., 2006; Sato and Yamaji, 2006). Several strategies have been proposed to solve this problem, but in general all the methods try to find stress tensors which are capable of explaining a maximal possible proportion of the fault-slip data observed in the field. The tensors which explain the greatest percentage of slip data are taken to be favoured candidates for the real paleostresses. This process is repeated until no physically meaningful stress tensor can be calculated from the remaining data.

Another philosophy of paleostress analysis of heterogeneous fault-slip data was introduced by, for example, Simón-Gómez (1986), Nemcok and Lisle (1995), Nemcok et al. (1999) and Yamaji (2003). These authors described methods, which allow faults to be separated into homogeneous subsets prior to stress inversion. On the Simón-Gómez's Y−R diagram faults are graphically shown as curves, and faults belonging to the same homogeneous subset are identified by a common intersection of their respective curves. Nemcok and Lisle (1995) describe a method which is based on the evaluation of numerical attributes of fault-slip data, relating them to all possible stress tensors, and then apply a clustering method to group the data into homogeneous subsets. This method was further improved by Nemcok et al. (1999) by combining cluster analysis with the right-dihedra method of Angelier and Mechler (1977). Yamaji (2000a,b, 2003) proposed a different clustering technique where the data are divided into k-element subsets to which the ordinary inversion technique is applied. Significant solutions are identified as clusters in a four-dimensional parameter space. In addition, the reliability of each stress is indicated by the density of the cluster.

A special type of cluster analysis of heterogeneous fault-slip data is based on the Fry's (1999) sigma space concept. Such methods were proposed and discussed by Fry (1999, 2001), Shan et al. (2003, 2004, 2006) and Sato and Yamaji (2006). Their benefit is that the paleostress inversion technique becomes linear in the most part after the transformation from the three-dimensional space to the six-dimensional sigma space (Fry, 1999; Shan et al., 2006). In sigma space, fault-slip data are transformed into datum vectors (f-poles) that, if homogeneous, tend to lie *in* or *near* a hyperplane (a higher dimension analogue of a 2D plane or 3D space) crossing the origin (Fry, 1999). Geometrically, in sigma space, the stress vector is perpendicular to the datum vector. Therefore, the normal to the hyperplane containing datum vectors is the optimal stress vector representing the optimal stress tensor (Shan et al., 2006). Since the basic Fry's technique is only suitable for analyzing homogeneous fault-slip data, Shan et al. (2003) presented an objective function algorithm (OFA) on the basis of hard division by utilizing modern clustering analysis. This technique has the ability to separate polyphase fault-slip data by detecting linear structures existing in the fault-slip data representation in the sigma space.

In this paper, we describe the *Gauss method* for separation of heterogeneous fault systems into the homogeneous fault subsystems. The method is based on the traditional philosophy of fault-slip data inversion, which involves the concept of the best-fit stress tensor. First, the *compatibility function* is defined as a Gaussian function, which depends on the *compatibility measure*, taking into account both (1) the angular misfit between the resolved shear stress and actual direction of movement on the fault plane, and (2) the ratio between the normal and shear stress on that fault plane, since it is assumed that the results of paleostress inversion should be in agreement with the Amonton's Law. Both the compatibility function and compatibility measure represent a measure of correspondence between some trial stress tensor and fault-slip datum. The optimal stress tensors for each homogeneous subsystem of faults are found by maximizing the object function, which is defined through a summation of the compatibility functions for all fault-slip data. We propose that the topography of the object function and its global and highest local maxima reflect different stress regimes that influenced and activated the faults. The aim of this paper is to verify the reliability of the Gauss method by mathematical means and numerical tests, and to analyse its effectiveness in the case of large dispersion of angular misfit between the direction of movement and resolved shear stress along the faults.

2. The Gaussian compatibility function

One of the basic assumptions of paleostress analysis is that of parallelism between the direction of movement and the

shear stress along the fault, which can be mathematically expressed as (Wallace, 1951; Bott, 1959):

$$\vec{s} \| \vec{\tau} = \boldsymbol{\sigma}\vec{n} - (\boldsymbol{\sigma}\vec{n}\cdot\vec{n})\vec{n}, \tag{1}$$

where $\vec{s}$ is the direction of slip, $\vec{\tau}$ is the shear stress, $\boldsymbol{\sigma}$ the stress tensor and $\vec{n}$ normal vector to the fault plane. First, it is necessary to introduce the convention of the sign. The one which will be used here is that the stresses are taken positive when compressive and negative when tensional. This is opposite to the convention adopted in works on the theory of elasticity and continuum mechanics, however, it is more convenient to have compressive stresses positive, since in the Earth's crust the compressive stresses prevail (Jaeger and Cook, 1969; Sibson, 1985, 1989; Ranalli, 2000; Ranalli and Yin, 1990; Yin and Ranalli, 1992, 1995). The eigenvalues of the stress tensor are denoted by σ_1 (maximum stress magnitude), σ_2 (intermediate stress magnitude) and σ_3 (minimum stress magnitude), where $\sigma_1 \geq \sigma_2 \geq \sigma_3$. Because of the natural dispersions, the direction of slip is generally supposed to be nonparallel to the shear stress. The angle between the direction of slip $\vec{s}$ and shear stress $\vec{\tau}$ will be denoted by α. The distribution of α for a given fault population is unknown, but for the sake of simplicity it will be approximated here with the Gaussian distribution:

$$f(\alpha) = \frac{1}{\sqrt{2\pi}s_0}\exp\left(-\frac{\alpha^2}{2s_0^2}\right), \tag{2}$$

where s_0 represents the dispersion of the distribution. The probability for the angular misfit to lie somewhere between $\alpha - \Delta\alpha$ and $\alpha + \Delta\alpha$ is approximately $f(\alpha)\cdot 2\Delta\alpha$, and the corresponding number of faults with such a misfit is $Nf(\alpha)\cdot 2\Delta\alpha$, where N is the total number of faults. The Gaussian function may be used as *a criterion of compatibility* of a fault with a given stress tensor $\boldsymbol{\sigma}$. Let us define the *compatibility function*:

$$w_i = \exp\left(-\frac{\alpha_i^2}{2s^2}\right). \tag{3}$$

Here i denotes the fault number, and s is a parameter, which represents the value of the second moment (=dispersion parameter) of the distribution of angular misfit between the shear stress and actual direction of slip along the faults. Optimally, its value should be equal to s_0. In the inversion process, we usually do not know the correct value of s_0 prior to calculation. Therefore a slightly different value of the parameter s with respect to s_0 is generally used in the first step. When the direction of the slip $\vec{s}$ is parallel to the direction of the shear stress $\vec{\tau}$, characterized by $\alpha_i = 0$, the value of compatibility function w_i equals 1. However, when the direction of movement along the fault is oblique to the direction of the shear stress, the value of the compatibility function is less than 1. In the ideal case, a given stress tensor $\boldsymbol{\sigma}$ gives high values of compatibility function for all faults. Such stress tensor can be found using the *object function*:

$$F = \sum_{i=1}^{N} w_i. \tag{4}$$

The value of this object function depends on the distribution $f(\alpha)$ and on the parameter s in the Eq. (3). For the optimal stress tensor, the object function can be approximated with an integral:

$$F = \sum_{i}^{N} w_i \approx \frac{N}{\sqrt{2\pi}s_0}\int_{-\pi}^{\pi}\exp\left(-\left[\frac{\alpha^2}{2s_0^2}+\frac{\alpha^2}{2s^2}\right]\right)\mathrm{d}\alpha$$

$$\approx \frac{N}{\sqrt{2\pi}s_0}\int_{-\infty}^{\infty}\exp\left(-\left[\frac{\alpha^2}{2s_0^2}+\frac{\alpha^2}{2s^2}\right]\right)\mathrm{d}\alpha = \frac{N}{\sqrt{s_0^2/s^2+1}}. \tag{5}$$

If we choose $s \ll s_0$, then only faults for which $\alpha_i \approx 0$ contribute to the value of the object function F. It is supposed that the number of such faults is low, thus the value of F will be low as well.

In the opposite case we can take a large value of the parameter s, and the value of compatibility function becomes approximately 1 for each fault, thus $F \approx N$.

In the ideal case, we can assume that $s = s_0$. In this case, the value of the compatibility function is close to 1 only when directions of movement and the shear stress are parallel. Faults with compatibility function approximately equal to 1 are considered as compatible with a chosen stress tensor $\boldsymbol{\sigma}$. All other faults are incompatible with this stress tensor and do not contribute considerably to the value of the object function F. When $s = s_0$, the object function F equals $F \approx N/\sqrt{2}$.

The fact that the object function F depends on the stress tensor $\boldsymbol{\sigma}$ can be effectively used in the inverse problem. For a randomly chosen stress tensor $\boldsymbol{\sigma}$, not capable of explaining slip patterns on observed faults, it is supposed that the value of object function F will be low, attaining a much lower value than for the optimal tensor $\boldsymbol{\sigma}_t$:

$$F(\boldsymbol{\sigma}) \ll F(\boldsymbol{\sigma}_t). \tag{6}$$

We assume that the optimal stress tensor should be found by maximizing the object function F:

$$F(\boldsymbol{\sigma}_t) = \max. \tag{7}$$

For large values of the parameter s such statement is equivalent to the least-mean-square optimization, $\sum_i \alpha_i^2 = \min$, because:

$$w_i = \exp\left(-\frac{\alpha_i^2}{2s^2}\right) \approx 1 - \frac{\alpha_i^2}{2s^2} + \cdots \tag{8}$$

Therefore the object function can be written as:

$$F = \sum_{i=1}^{N}\left(1 - \frac{\alpha_i^2}{2s^2} + \cdots\right) \approx N - \frac{1}{2s^2}\sum_{i=1}^{N}\alpha_i^2 = \max, \tag{9}$$

which is equivalent to $\sum_i \alpha_i^2 = \min$. Thus, when the chosen value of the parameter s is large, the maximization of the object function F leads to a stress tensor capable of explaining the slip pattern on all faults observed in the rock mass. However, such a stress tensor does not exist when we deal with a heterogeneous fault system. Instead, we assume that by choosing some appropriate value of parameter s, all the stress

tensors that influenced the fault system could be determined by finding the global and highest local maxima of the object function F.

3. The topography of the object function

In this section, a firmer mathematical consideration is proposed to verify the reliability of using the Gauss method for paleostress analysis of heterogeneous fault-slip data. Let us have a heterogeneous fault system consisting of N faults that belong to two homogeneous fault subsystems of N_1 and N_2 faults. The corresponding stress tensors of the first and the second stress regime will be denoted as $\boldsymbol{\sigma}_1$ and $\boldsymbol{\sigma}_2$, respectively. We can assume that the following relations hold:

$$\begin{aligned} F(\boldsymbol{\sigma}_1) &\approx \tfrac{N_1}{\sqrt{2}} + \Delta(N_2), \\ F(\boldsymbol{\sigma}_2) &\approx \tfrac{N_2}{\sqrt{2}} + \Delta(N_1). \end{aligned} \tag{10}$$

Here $\Delta(N_2)$ and $\Delta(N_1)$ represent the influence of faults of the second homogeneous fault system on the value of the object function in the local maximum corresponding to the first stress state, and *vice versa*. For a randomly chosen and non-optimal stress tensor $\boldsymbol{\sigma}$ it is expected that the value of the object function will be $F(\boldsymbol{\sigma}) \ll F(\boldsymbol{\sigma}_1), F(\boldsymbol{\sigma}_2)$. However, this can only be true when the parameter s has some appropriate value. Let us now consider how the value of this parameter should be chosen.

First, we will analyse an ideal heterogeneous fault system, where all natural dispersions are absent, so that $s_{0,1} = 0$ and $s_{0,2} = 0$. In this case, we expect the following relation to be true:

$$F(\boldsymbol{\sigma}) \geq N_j, \quad \text{when } \boldsymbol{\sigma} = \boldsymbol{\sigma}_j, \text{ for every } s. \tag{11}$$

Here j denotes an index of the homogeneous fault subsystem. Now, we take a minimal nonzero angular misfit between the actual direction of slip and shear stress for some randomly chosen stress tensor, $\alpha_{\min} = \min\{\alpha_1, \alpha_2, \ldots, \alpha_N\}$ so that $\alpha_{\min} \neq 0$, and the following relation follows for the object function:

$$\begin{aligned} F(\boldsymbol{\sigma}) &= \sum_{i=1}^{N} \exp\left(-\frac{\alpha_i^2}{2s^2}\right) \leq \sum_{i=1}^{N} \exp\left(-\frac{\alpha_{\min}^2}{2s^2}\right) \\ &= N \exp\left(-\frac{\alpha_{\min}^2}{2s^2}\right). \end{aligned} \tag{12}$$

Considering the statement:

$$N \exp\left(-\frac{\alpha_{\min}^2}{2s^2}\right) < K \ll N_j, \tag{13}$$

where K is some suitably chosen value much lower than N_j, we find:

$$s < \left(\frac{1}{2\ln(N/K)}\right)^{1/2} \alpha_{\min}. \tag{14}$$

This equation suggests that for every randomly chosen stress tensor such a value of parameter s exists, that for the object function F the relation $F(\boldsymbol{\sigma}) \ll N_j$ holds, where N_j represents the number of faults of jth homogeneous fault subsystem. This proves the tested assumption at least in the case of optimal fault-slip data with no angular dispersion. For some appropriate value of the parameter s, the global and highest local maxima of the object function F are defined by optimal stress tensors corresponding to individual homogeneous fault subsystems, since for such stress tensors the value of the object function is equal to N_j or even larger (Eq. (11)).

Now, we consider a second example, where we deal with non-optimal heterogeneous fault-slip data with a considerable angular misfit (noise) between theoretical and real direction of slip. First, for an individual homogeneous fault-subset consisting of N_j faults we will define the average angular misfit $\overline{\alpha}$ predicted by some non-optimal stress tensor $\boldsymbol{\sigma}$, and the standard deviation of angular misfit predicted by this tensor will be denoted as s_0. Note that the standard deviation s_0 is related to the angular difference between angular misfit α and average angular misfit $\overline{\alpha}$. It is supposed that for every (jth) homogeneous subset the standard deviation of angular misfits s_0 predicted by non-optimal stress tensor is larger than standard deviation s_j predicted by the optimal stress tensor $\boldsymbol{\sigma}_j$ corresponding to this, jth, subset. Generally, the distribution $f(\alpha)$ of angular misfits for non-optimal stress tensor is not known. It does not necessarily follow a Gaussian distribution and may be highly dependent on a given data set and trial stress tensor. However, for the sake of simplicity, we will approximate this distribution with a Gaussian function in a way that the following relation holds:

$$N_j f(\alpha) \leq \frac{K}{\sqrt{2\pi}s_0} \exp\left(-\frac{(\alpha - \overline{\alpha})^2}{2s_0^2}\right), \tag{15}$$

where K has some suitable chosen value in order to warrant the above relation to be true. If the distribution $f(\alpha)$ would ideally follow the Gaussian distribution, then K should be equal to N_j, but in general, it can have any value, depending on the unknown distribution $f(\alpha)$. It is possible that for heterogeneous faults-slip data the value of K could be even larger than N_j, because the faults belonging to other homogeneous subsets are also present. The value of the object function can be now estimated as (see Appendix A):

$$\begin{aligned} F &\approx \frac{K}{\sqrt{2\pi}s_0} \int_{-\pi}^{+\pi} \exp\left(-\left(\frac{(\alpha - \overline{\alpha})^2}{2s_0^2} + \frac{\alpha^2}{2s^2}\right)\right) \mathrm{d}\alpha \\ &\leq \frac{K}{\sqrt{s_0^2/s^2 + 1}} \exp\left(\frac{\pi^2}{s_0^2}\right) \exp\left(-\frac{\overline{\alpha}^2}{2s_0^2}\right). \end{aligned} \tag{16}$$

The ratios s_0/s, π/s_0 and $\overline{\alpha}/s_0$ control the resolution of the Gauss method. If some non-optimal stress tensor predicts large angular deviations with large standard deviation s_0 with respect to the value of the parameter $s = s_{0,j}$ (which is used in the calculation) for all homogeneous subsets present in the heterogeneous data, then the value of the object function

will certainly be low, because the factor $\sqrt{s_0^2/s^2+1}$ will have a large value. Additionally, the object function decreases with increasing value of $\overline{\alpha}$. This again suggests that even in the case of large angular misfits, for the appropriate value of the parameter s the global and highest local maxima of the object function F are defined by optimal stress tensors corresponding to individual homogeneous fault subsystems, because for those tensors the value of the object function will be large. However, problems may appear when different optimal stress tensors, which actually induced slips along the faults, are similar to each other in the sense of orientation of stress axes. Then some intermediate non-optimal stress tensors could predict $s_0 \approx s_{0,j} = s$ and lower average angular misfits $\overline{\alpha}$ than $s_{0,j}$ for all homogeneous subsets. In this case the position of prominent maxima of the object function could be misplaced with respect to the solutions for the real stress tensors $\boldsymbol{\sigma}_j$, especially if K is larger than N_j. Then unexpected solutions could appear.

4. Mechanically acceptable compatibility measure and compatibility function: the Gauss method

Several studies (e.g., Reches, 1987; Angelier, 1989; Reches et al., 1992; Yin and Ranalli, 1995; Fry, 2001) suggest that one of the greatest shortcomings of the paleostress inversion methods is that the results can be often mechanically unacceptable, giving low value of shear stress and high value of normal stress on the fault planes. Such solutions are not in agreement with the Amonton's Law, which states (e.g., Jaeger and Cook, 1969; Angelier, 1989):

$$\tau \geq \mu\sigma_n = \tan\phi_2 \cdot \sigma_n, \tag{17}$$

where μ is the coefficient of residual friction for sliding on a preexisting fault, and σ_n is the normal stress on the fault. The physical meaning of this law is that the fault plane is activated only when shear stress exceeds some critical value $\mu\sigma_\mathrm{n}$, which represents the frictional shear strength. In the Mohr diagram (Fig. 1) the points which represent the values of normal and shear stress on the faults (the term "Mohr points" will be used here for these points) lie above the straight line $\tau = \mu\sigma_n = \tan\phi_2 \cdot \sigma_n$. The stresses in the Earth crust related to faulting are usually compressive (Jaeger and Cook, 1969; Sibson, 1985, 1989; Ranalli, 2000; Ranalli and Yin, 1990; Yin and Ranalli, 1992, 1995), thus the area on the Mohr diagram, where the "Mohr points" can lie, is located below the straight line $\tau = \tan\phi_1 \cdot \sigma_n$, which represents the tangent of the largest Mohr circle on the Mohr diagram (Fig. 1). The parameter ϕ_1 roughly approximates the value of the angle of internal friction. This angle constrains the shear strength of an intact rock, which can be approximated by the Coulomb–Navier shear failure criterion (e.g., Jaeger and Cook, 1969; Ranalli and Yin, 1990):

$$\tau = S + \sigma_n \cdot \tan\phi_i. \tag{18}$$

Here, S and ϕ_i are the cohesive strength and the angle of internal friction, respectively. When cohesion S is small, the value of parameter ϕ_1 is approximately equal to the angle of internal friction ϕ_i, but generally ϕ_1 has a larger value with respect to ϕ_i.

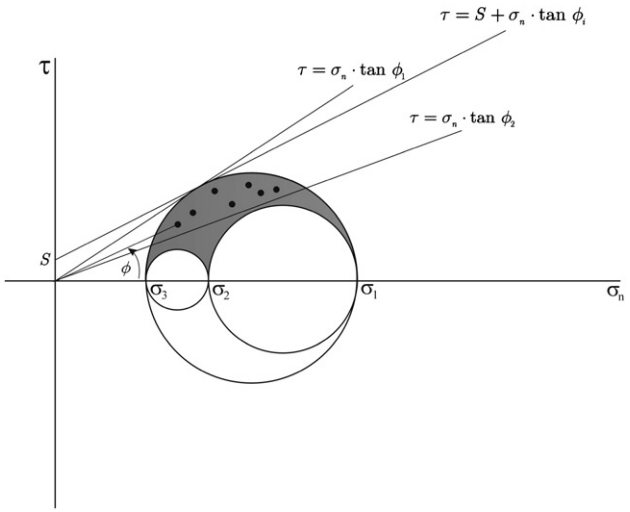

Fig. 1. Mohr diagram illustrating normal σ_n and shear stress τ on the faults (black "Mohr points"). σ_1, σ_2 and σ_3 represent principal stress magnitudes and S is the cohesion. The position of the "Mohr points" for all possible orientations of the faults is restricted to the gray area. However, for mechanically acceptable solutions the position of "Mohr points" is additionally restricted to the area between the two straight lines with equations $\tau = \sigma_n \cdot \tan\phi_1$ and $\tau = \sigma_n \cdot \tan\phi_2$. The first represents the tangent of the largest Mohr circle and roughly approximates the angle of internal friction ϕ_i for an intact rock, and the second represents the Amonton's Law.

The correct solutions of the paleostress analysis should satisfy mechanical conditions as discussed above, and should therefore be of the form:

$$\boldsymbol{\sigma}_t = \mathrm{konst} \cdot \boldsymbol{\sigma}_t^{(\mathrm{orig.})}, \tag{19}$$

where $\boldsymbol{\sigma}_t^{(\mathrm{orig.})}$ is the true stress tensor, which describes actual stress state in the time of faulting, and $\boldsymbol{\sigma}_t$ is our solution. When additional mechanical conditions are considered in the stress inversion approach, the results should then generally constrain both the Bishop's (1966) stress parameter $\Phi = (\sigma_2 - \sigma_3)/(\sigma_1 - \sigma_3)$ and the ratio between the eigenvalues of the stress tensor, $\sigma_1 : \sigma_2 : \sigma_3$ (e.g., Angelier, 1989).

Based on the above discussion, we put the additional conditions on the mechanical acceptability of the solutions into the compatibility function. First we define the *compatibility measure,* which considers both the angular misfit α_i between the predicted and actual direction of slip on the fault, and the position of the "Mohr point" on the Mohr diagram:

$$\delta_i^2 = \alpha_i^2 + \left(w_{2,i}|\phi - \phi_2|\frac{2\Delta}{\phi_2}\right)^2 + \left(w_{1,i}|\phi - \phi_1|\frac{2\Delta}{\phi_1}\right)^2, \tag{20}$$

where parameters $w_{1,i}$ in $w_{2,i}$ are as follows:

$$\begin{aligned} w_{2,i} &= 1, \quad \text{when } \phi < \phi_2, \\ w_{2,i} &= 0, \quad \text{when } \phi \geq \phi_2, \end{aligned} \tag{21}$$

and

$$\begin{aligned} w_{1,i} &= 1, \quad \text{when } \phi > \phi_1, \\ w_{1,i} &= 0, \quad \text{when } \phi \leq \phi_1. \end{aligned} \tag{22}$$

The angle of friction ϕ for an individual fault is measured between the σ_n axis on the Mohr diagram and the line which connects the "Mohr point" and the origin of the Mohr diagram (Fig. 1). The parameters ϕ_1 and ϕ_2 constrain the possible values of the ratio between the normal and shear stress on the faults, and therefore favour mechanically acceptable solutions of the inverse problem. The parameter ϕ_2 represents the angle of residual friction for sliding on a preexisting fault; $\phi_2 = \arctan(\mu)$, and the parameter ϕ_1 roughly approximates the angle of internal friction ϕ_i for an intact rock. The optimal values of these parameters for different rocks and granular materials can be found in the tables (e.g., Jaeger and Cook, 1969; Schellart, 2000). Since the angle of internal friction ϕ_i generally has a higher value with respect to the angle of residual friction ϕ_2, the value of the parameter ϕ_1 should be slightly higher than ϕ_2. The parameter ϕ_2 therefore constrains the lowest possible value for the angle of friction on the preexisting fault and the parameter ϕ_1 represents the highest possible value for the angle of friction on the preexisting fault.

The parameter Δ represents a threshold value for the compatibility measure δ_i. Only the stress tensors that explain the direction of slip on a given fault and position of its "Mohr point" on the Mohr diagram with the compatibility measure δ_i lower than the selected threshold Δ, are considered to be compatible with the observed fault-slip datum. Now, we also redefine the compatibility function:

$$w_i = \frac{1}{1-\exp\left(-\Delta^2/2s^2\right)}\left(\exp\left(-\frac{\delta_i^2}{2s^2}\right)-\exp\left(-\frac{\Delta^2}{2s^2}\right)\right), \quad \text{when } \delta_i < \Delta w_i = 0, \quad \text{when } \delta_i \geq \Delta. \tag{23}$$

The compatibility function defined in such way is graphically presented in Fig. 2. Such a definition is considerably more useful than the one from Eq. (3), since only the faults that eventually are compatible with the chosen stress tensor contribute to the value of the object function F. Ideally, for all the outliers the value of compatibility function should be zero, since it is supposed that the outliers either belong to some other homogeneous fault subsystem or represent the faults influenced by local stress fields. The values of parameters s and Δ depend on the inhomogeneity of the stress field at the time of faulting. When the stress field at the time of faulting was highly inhomogeneous, the values of s and Δ should be large enough, for example $s \geq 30°$ and $\Delta \geq 60°$. If the stress field was less inhomogeneous, lower values could be used, for example $s \geq 15°$ and $\Delta \geq 30°$. The inversion procedure should be repeated many times using different values of the parameters s and Δ in order to find the best stress tensor solutions for each homogeneous fault subsystem. The optimal solutions are identified when the calculated standard deviation of angular misfit s_0 and maximal angular misfit α_{max} predicted by the given stress tensor solution are approximately equal to the values of s and Δ used in the inversion.

5. Testing the method

Our method has been implemented in the T-TECTO computer program. The demo version of T-TECTO can be obtained free of charge on the following website: http://www2.arnes.si/~jzaloh/t-tecto_homepage.htm. Based on the grid-search method, this program analyses the topography of the object function F and searches for its global and highest local maxima using the definitions of compatibility measure and compatibility function presented in Eqs. (20) and (23). All possible trial stress tensors are calculated in the following way: first the dip angle of maximum stress axis σ_1 is defined ranging from 2° to 89° with the resolution of 5°. For each dip angle, the dip direction is calculated increasing from 2.5° to 360° at regular intervals of $(90°/(90° - \text{dip})) \times 5°$. Secondly, the σ_2 and σ_3 axes are rotated in the plane perpendicular to each σ_1-axis in the clockwise sense for 180° at regular intervals of 5°. The resolution of the stress parameter Φ in the current version of the program T-TECTO is 0.1, so that 11 values of this parameter are assigned to each orientation of stress axes.

The method uses four specific parameters; s, Δ, ϕ_1 and ϕ_2, where each stress tensor has its own associated values of these parameters. The optimal stress tensors corresponding to different homogeneous subsystems are found in the following steps:

- *step 1*: after finding the global maximum of the object function and the corresponding stress tensor, the program searches for faults compatible with the obtained stress tensor. Only faults with angular misfits lower than $\alpha_{max,1} \approx \Delta$ are considered to be compatible.

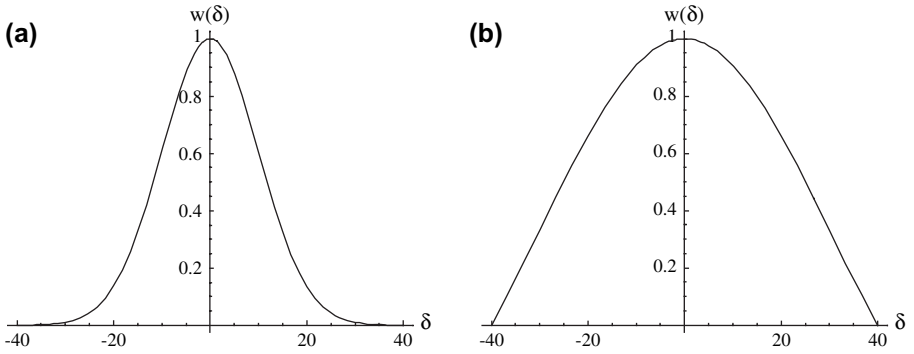

Fig. 2. The compatibility function $w(\delta)$ for two different values of parameter s; (a) $\Delta = 40°$, $s = 10°$; (b) $\Delta = 40°$, $s = 30°$.

- *step 2*: in the second step only the faults that are incompatible with the first stress tensor are analysed. Again, the global maximum of the object function is found, leading to the second stress tensor. The program verifies which faults are compatible with this stress tensor for angular misfits lower than $\alpha_{max,2} \approx \Delta$, however, now also the faults compatible with the first stress tensor are considered.
- *step 3*: the solution for the second stress tensor is refined by repeating the calculation of the maximum of the object function including all the faults that were found to be compatible in step 2. The global maximum found in steps 2 and 3 is equivalent to one of the highest local maxima of the object function when analyzing all fault-slip data together.

These three steps enable separation of two homogeneous fault subsystems. If additional homogeneous subsystems are present, the procedure can be repeated until all subsystems are found. For each solution we determine the following:

- N_i – the number of correctly separated faults corresponding to the ith stress tensor.
- N_i^D – the number of faults classified as compatible with the ith stress tensor but actually not belonging to it.

We tested the efficiency of the Gauss method by analyzing artificial heterogeneous fault systems generated with computer program AmontonWin. The program generates a prescribed number of randomly oriented faults or faults with a chosen orientation, and calculates the direction of movement on those faults according to the stress tensor defined by the user. Such a procedure is often referred to as *a direct problem* (e.g., Fleischman and Nemcok, 1991; Angelier, 1994). Angular misfits between the resolved shear stress and direction of movement along the generated faults can be added, so that the effect of dispersion of these angular misfits on the effectiveness of the stress inversion method can be analysed. One of the basic assumption of the Gauss method is that the distribution of the angular misfits can be approximated with the Gaussian distribution. However, because of the errors in the estimation of the fault dip direction, the fault dip angle, striation pitch and the effect of inhomogeneity of the stress field at the time of faulting, the distribution of angular misfits may considerably deviate from the Gaussian distribution. Therefore, random angular misfits between theoretical and real direction of slip were introduced into our artificial data, representing even worse scenarios for the Gauss method to work properly.

5.1. Test 1 (a)

For Test 1 (a) we generated a homogeneous set of 75 randomly oriented fault-slip data compatible with the strike-slip stress regime with maximal compression $\vec{\sigma}_1$ in the N–S direction and minimal compression $\vec{\sigma}_3$ in the W–E direction (Fig. 3a). The value of the stress parameter Φ was set to 0.4. Since we were particularly interested in the effectiveness of our method when dispersion of angular misfit between the direction of slip and shear stress along the faults is large, random angular misfits were introduced in the data set with the maximum possible misfit angle set to 40°. The value of parameter ϕ_1 was set to 56°, and of parameter ϕ_2 to 20°.

The second homogeneous set and corresponding stress tensor were then generated by rotating the first set and stress tensor around the vertical axis for angle $\phi = 45°$ in the CW sense. The final heterogeneous system of 150 faults thus consists of two homogeneous subsystems of 75 faults (Fig. 3a), with 45° difference in the orientation of $\vec{\sigma}_1$ and $\vec{\sigma}_3$ stress axes.

The fault-slip data were analysed with the T-TECTO program using the following values of parameters: $\phi_1 = 56°, \phi_2 = 20°$, $s = 10°$, $\Delta = 30°$ and $\alpha_{max,1} = \alpha_{max,2} = 50°$. The program successfully separated the two fault subsystems, and their respective stress tensors (the direction of stress axes and ratio between the principal stresses) were correctly determined. The results are graphically presented in Fig. 3b. All 75 faults of the second subsystem and 74 faults of the first subsystem were found, thus the program failed to correctly interpret only a single fault. Since large dispersion of angular misfit between the direction of slip and shear stress along the faults was prescribed during the fault generation, some faults were determined compatible with both stress tensors, namely $N_1^D = 7$ and $N_2^D = 10$ for $\alpha_{max,1} = \alpha_{max,2} = 50°$.

We ran several additional tests, but now varying the angular difference φ in the orientation of stress axes $\vec{\sigma}_1$ and $\vec{\sigma}_3$ belonging to the two homogeneous fault subsystems. Results are presented in Table 1 (a). When angular difference φ was lower than 25°, the program was not able to recognize heterogeneity of the fault system and treated the data as homogeneous. Obviously the angular misfits introduced in the data were too high for the two subsystems to be separable. As soon as the angular difference φ was 25° or higher, the effectiveness of the method increased greatly and the number of faults found compatible with both stress tensors decreased rapidly as well (Table 1 (a)).

5.2. Test 1 (b)

Even better results were obtained when there were no angular misfits between the direction of slip and shear stress in the data set. In this test we used the following values of parameters: $s = 30°$, $\Delta = 5°$, $\phi_1 = 56°$ and $\phi_2 = 20°$. The results are shown in Table 1 (b). Here a 100% effectiveness of the method was reached already for angular difference $\varphi = 10°$, and the number of faults considered compatible with both stress tensors for $\alpha_{max,1} = 10°$ and $\alpha_{max,2} = 15°$ was low in all cases.

5.3. Test 2

In this test, we analysed a more realistic example of a heterogeneous fault system consisting of three homogeneous fault subsystems (Fig. 4a). In order to verify the influence of uneven size of different homogeneous subsystems on the effectiveness of the inversion method, different numbers of faults were generated for the second homogeneous subsystem with respect to the other two subsystems. The first homogeneous subsystem of 25 faults was produced by a strike-slip stress regime with

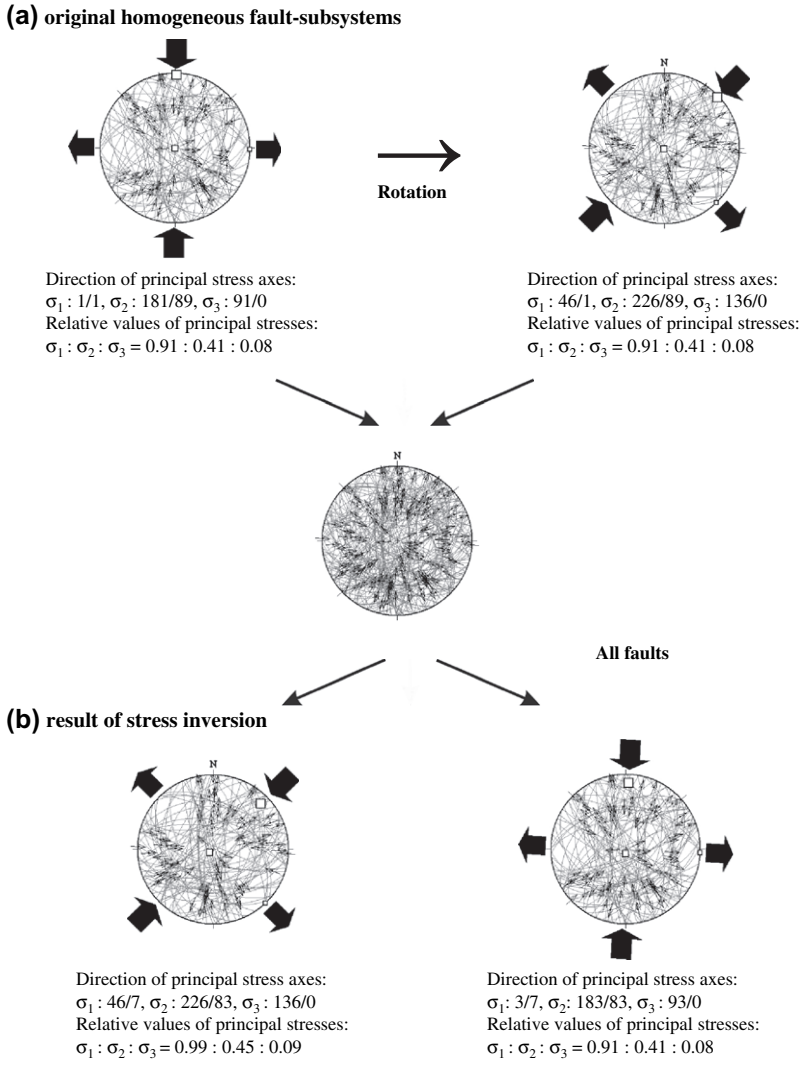

Fig. 3. (a) Synthetically generated homogeneous fault subsystems analysed in the Test 1 and the corresponding stress axes (Schmidt net, lower hemisphere); (b) results of the stress inversion and fault separation by using the Gauss method.

maximal horizontal compression in the NW–SE direction with value of the stress parameter Φ set to 0.4. The second homogeneous subsystem of 50 faults was produced by a compressional stress regime with maximal horizontal compression in the N–S direction with value of the stress parameter Φ set to 0.4. The third homogeneous subsystem consists of 25 faults and was produced by an extensional stress regime with maximal compression in the vertical direction with value of the stress parameter Φ set to 0.1. In the fault-slip data generation procedure the maximal possible misfit angle between the slip direction and shear stress along the faults was limited to 20°. The value of parameter ϕ_1 was set to 56°, and of parameter ϕ_2 to 20°.

The fault-slip data have been analysed using the following values of parameters: $\phi_1 = 56°$, $\phi_2 = 20°$, $s = 50°$ and $\Delta = 30°$. The three determined stress tensors and the faults found compatible with them are presented in the Fig. 4b, and the number of faults assigned to each phase (the values of N_i and N_i^D) is listed in the Table 1 (c). The program successfully separated the three fault subsystems, and also their respective stress tensors (the direction of stress axes and ratio between the principal stresses) were successfully determined. Only six faults were not interpreted correctly by the program. The first processing step separated the faults belonging to the largest homogeneous subsystem, and the other two subsystems were determined in the following steps. Because of the angular misfits introduced when generating the fault-slip data, several faults were found compatible with more than one stress tensor. These faults had an apparent effect only on the determination of the stress parameter Φ for the third (extensional) stress regime. The original value of this parameter was 0.1, but the value calculated by the inversion method was 0.3.

6. Discussion

The methods for analysis of heterogeneous fault-slip data share several similar shortcomings. The most detailed analysis of limitations of these methods was described and discussed by Liesa and Lisle (2004) and Yamaji et al. (2006). Liesa and Lisle (2004) analysed the efficiency of the methods of Etchecopar et al. (1981), Yamaji (2000a,b) and the cluster

Table 1
Effectiveness of stress inversion and fault separation by using the Gauss method

Test 1 (a)						
φ	N_1	N_2	N_1^D	N_2^D	$\alpha_{max,1}$	$\alpha_{max,2}$
25	57	75	44	41	40	50
30	50	74	45	34	40	50
35	58	74	46	24	50	50
40	73	74	15	16	50	50
45	75	74	7	10	50	50
50	75	74	6	8	50	50
55	75	74	4	7	50	50
60	75	74	3	5	50	55
65	75	74	3	2	55	50
70	75	75	1	2	50	50
75	75	75	1	1	50	50
80	75	75	0	0	50	55
85	75	75	0	0	50	50
90	75	75	0	0	50	50
Test 1 (b)						
φ	N_1	N_2	N_1^D	N_2^D	$\alpha_{max,1}$	$\alpha_{max,2}$
10	75	75	17	8	10	15
15	75	75	11	10	10	15
20	75	75	6	4	10	15
25	75	75	3	3	10	15
30	75	75	3	2	10	15
35	75	75	0	0	10	15
40	75	75	0	0	10	15
Test 2						
Index of the subsystem			N_i		N_i^D	$\alpha_{max,i}$
1			48 (of 50)		1	25
2			24 (of 25)		5	30
3			24 (of 25)		14	30

φ is the angular difference between the direction of principal stress axes $\vec{\sigma}_1$ and $\vec{\sigma}_3$ of the two stress tensors used to generate the synthetic fault data. N_i is the number of correctly separated faults corresponding to the ith stress tensor. N_i^D is the number of faults classified as compatible with the ith stress tensor but actually not belonging to it. Only faults with angular misfits lower than $\alpha_{max,i}$ are considered to be compatible with the ith stress tensor. See text for details.

procedure of Nemcok and Lisle (1995), but the results can probably be extrapolated to other methods based on similar assumptions. The key problems that influence the success of the paleostress inversion are related to: (1) the choice of the deviation threshold angle between the real and theoretical slip direction, (2) similarity between different stress tensors that induced slips along the faults, (3) uneven size of homogeneous subsets, (4) mechanical acceptability of the solutions, and (5) measurement errors and inhomogeneity of the stress field at the time of faulting.

6.1. Choice of the deviation threshold angle

As shown by Liesa and Lisle (2004), the choice of the misfit threshold angle between the real and theoretical slip direction significantly influences the final results of the methods, which use the threshold angle as a parameter. For example, in the cluster procedure of Nemcok and Lisle (1995) a very small value of the threshold angle (about 6° or less) tends to excessively fragment the fault-slip data, producing an unrealistically large number of similar paleostress tensors, whereas a larger value (15° or more) leads to misgrouping of the data. In the Gauss method the threshold angle is accounted for in the parameter Δ, which has a direct effect on the summation in the object function. Small value of Δ influences the results in the same way as the deviation threshold angle in the cluster procedure of Nemcok and Lisle (1995). However, when the value of Δ is unrealistically large, the misgrouping of faults can still be avoided by choosing appropriate values of other three parameters, s, ϕ_1 and ϕ_2.

6.2. Similarity between the stress tensors

Separating individual stress tensors from polyphase fault-slip data sets is least effective when stress tensors that induced slips along the faults are similar in orientation of stress axes and in the value of stress ratio. In this case, the separation algorithms can easily lead to spurious, hybrid solutions (Nemcok and Lisle, 1995). Liesa and Lisle (2004) demonstrated that the difference in orientation of stress axes of individual tensors should be at least 30° for separation techniques to be effective. Our numerical tests of the effectivity of the Gauss method confirm this for the case when there are large angular misfits between real and predicted slip directions in the data. However, when the angular misfits are very small or absent, the Gauss method is able to separate stress tensors even when their axes differ in orientation for as little as 10°.

6.3. Uneven size of homogeneous subsets

Difficulty of separating stress tensors generally increases when the homogeneous groups belonging to each tensor are very different in number of fault-slip data (Liesa and Lisle, 2004). The Etchecopar's method generally gives good results as long as the number of faults belonging to a particular stress tensor is sufficiently large relative to other stress tensors. Particularly when a stress tensor is defined by a small number of faults, the results might be numerically highly unstable due to the influence of faults belonging to other phases (Nemcok and Lisle, 1995; Liesa and Lisle, 2004). In this case several fault-slip data can be misclassified and explained by the other or non-optimal stress tensor. Orife and Lisle (2006) additionally warn that the stress tensors determined from a small number of faults (<9) should be treated with great caution, since in such a case seemingly satisfactory tensor solution can be found even for randomly generated faults.

The multiple-inverse method of Yamaji (2000a,b) also achieves satisfactory solutions only when the amount of data belonging to each homogeneous subset is roughly equal (Liesa and Lisle, 2004). In the opposite case the stress tensors defined by a small number of data are very difficult to detect because the number of combinations involving k faults of different homogeneous subgroups will be greater than the number of combinations involving k faults from the same homogeneous subset, leading to overabundance of intermediate solutions.

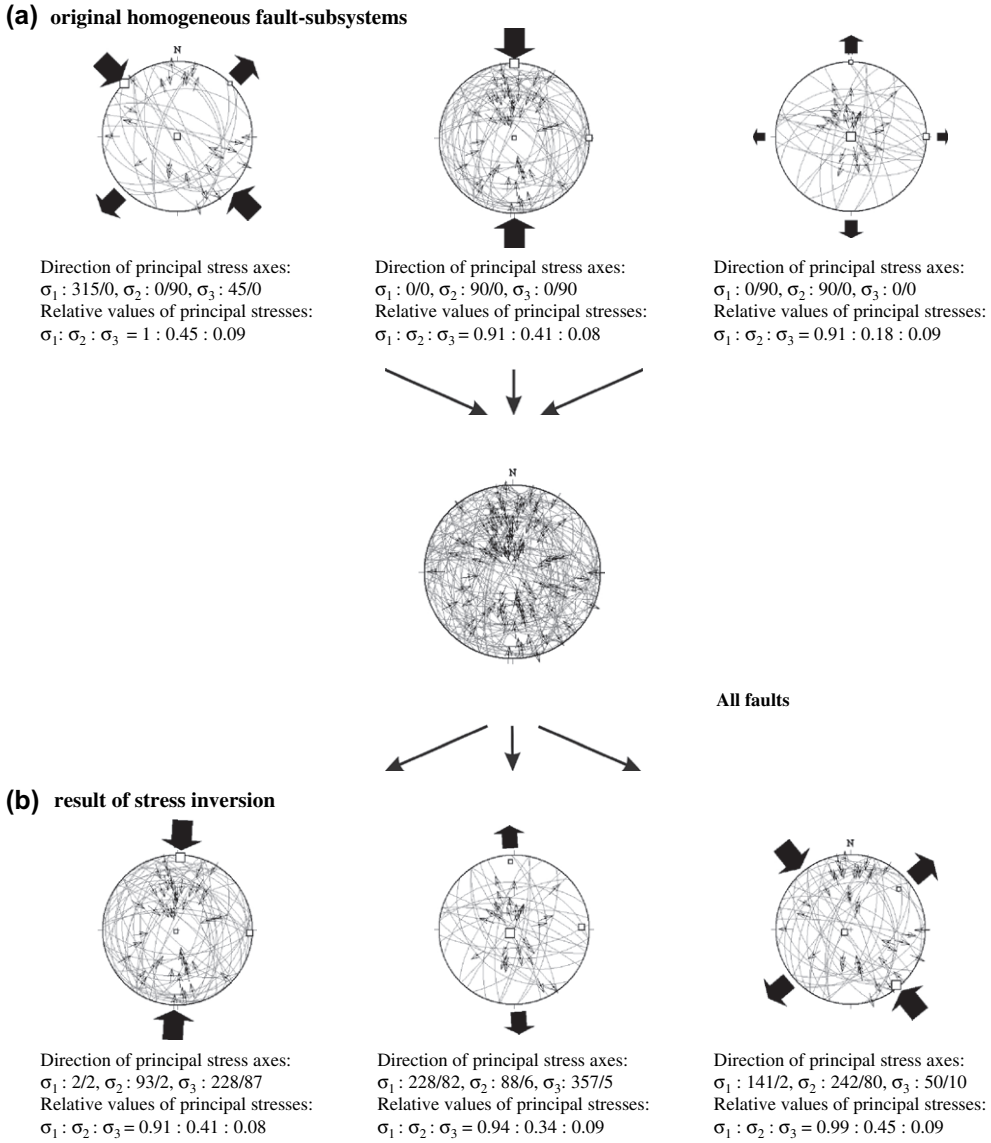

Fig. 4. (a) Synthetically generated homogeneous fault subsystems analysed in the Test 2 and corresponding stress axes (Schmidt net, lower hemisphere); (b) results of the stress inversion and fault separation by using the Gauss method.

Compared to the methods of Etchecopar and Yamaji, the Gauss method works well even when the number of faults belonging to separate stress tensors is very uneven. Problems may appear only for very small number of faults, because in this case the respective stress tensor solution is not sufficiently constrained. Another important advantage of the Gauss method is that it does not attempt to uniquely attribute each fault-slip datum to a single homogeneous subsystem. When large dispersions of angular misfit between the observed and theoretical direction of slip are present, some faults may be compatible with several stress tensors. Therefore, those faults cannot be uniquely prescribed to a single tectonic event, contrary to the basic assumption of most other methods.

6.4. Mechanical acceptability of the solutions

Many methods are problematic in this respect since they do not consider mechanical acceptability (i.e., the agreement with Amonton's Law) of the results at all (for example, the methods described by Etchecopar et al. (1981), Yamaji (2000a,b), Yamaji et al. (2006), Fry (1999, 2001) and Shan et al. (2003, 2004, 2006)). In the method of Etchecopar, mechanically incompatible faults may be manually removed from homogeneous subsets based on the position of their respective ''Mohr point'' on the Mohr diagram (Liesa and Lisle, 2004). Since the manual procedure is time-consuming and somewhat tedious, several authors introduced automated methods by incorporating additional parameters into the inversion algorithm. For example, Nemcok and Lisle (1995) defined a more sophisticated compatibility measure between the trial stress tensor and fault-slip data, which considers both the angular difference between the predicted and actual slip direction, and the user-chosen value of the shear stress ratio (the ratio between the shear and normal stress on the fault plane). The choice of the shear stress ratio strongly influences the mechanical interpretation and grouping of faults. When the shear stress ratio

is low (or is not considered at all), the algorithm groups the fault-slip data into subsets that can be preferentially explained as being formed due to fault reactivation. When a higher value of shear stress ratio is input, the fault-slip data are grouped into subsets explainable as newly formed faults (Liesa and Lisle, 2004). In the Gauss method, a similar approach is implemented by introducing the parameters ϕ_1 and ϕ_2. The two parameters constrain the possible values of the ratio between the normal and shear stress on the faults and therefore favour mechanically acceptable solutions of the inverse problem. Choosing large values of parameters ϕ_1 and ϕ_2 has the same effect as choosing a high shear stress ratio in the method of Nemcok and Lisle (1995); the same is true for small values.

6.5. Measurement errors and inhomogeneity of the stress field

Measurement errors and inhomogeneity of the stress field may significantly contribute to the misfit between the measured and theoretical slip direction. Shan et al. (2006) provide a detailed analysis of how this noise affects the paleostress inversion in the reduced sigma space. They generated numerous sets of homogeneous fault-slip data in extensional stress states and subsequently modified the data by adding a varying amount of measurement error of the striation pitch. Results demonstrated that the measurement errors greater than 10° may have a significant effect on estimated stress.

Our tests of the efficiency of the Gauss method give good and numerically stable results even in the case of extremely large random noise introduced into the data (as large as 40°). This indicates that numerical stability of the stress tensor solution is highly dependent on the inversion method used in the test. The main reason for the success of the Gauss method lies in the definition of the compatibility function, which is defined as a Gaussian function, so the function value is low for all faults influenced by local stress fields and for faults belonging to other stress phases. Therefore, the problematic data do not contribute considerably to the value of the object function in the maxima corresponding to the optimal stress tensor solutions. The main parameter controlling the influence of problematic faults is the parameter s, which represents the standard deviation of angular misfits between the theoretical and real direction of slip along the faults. Along with parameters Δ, ϕ_1 and ϕ_2, this parameter significantly controls the topography of the object function. The correct solutions can be obtained only if the values of the four parameters s, Δ, ϕ_1 and ϕ_2 are appropriately set. For example, for large values of parameter s and with no proposed deviation angular threshold Δ, the Gauss inversion method is equivalent to the least-mean-square optimization of the object function (Eq. (9)). Such approach is used in many traditional techniques (whether explicitly or implicitly). However, our mathematical analysis revealed that large values of parameter s are unsuitable when the fault-slip data are heterogeneous, which explains why the techniques based on least-mean-square optimization will be unsuccessful in analyzing such data.

7. Conclusions

Based on the results of performed tests we can conclude that the Gauss method is a highly effective and simple way of (1) separating heterogeneous fault systems into homogeneous subsystems and (2) calculating the respective stress tensor for each stress phase. Our method uses four parameters: s, Δ, ϕ_1 and ϕ_2, which need to be specified prior to calculation. All these parameters can significantly influence the topography of the object function F and therefore the obtained solutions. The topography of the object function F reflects the stress regimes that influenced and activated the faults only for appropriate values of the four parameters s, Δ, ϕ_1 and ϕ_2. In this case, the global and highest local maxima of the object function F determine the real solutions for the stress tensors. This was proved both by mathematical means and numerically by analyzing synthetical data sets. We demonstrated that the Gauss method gives good and numerically stable results even when relatively large dispersions of angular misfits between theoretical and real direction of slip are present in the data. The Gauss method has limitations only when the difference in orientation of stress axes between the separate stress states becomes too small. In such cases the prominent maxima of the object function may be misplaced with respect to the real solutions or the object function may have only one prominent maximum. Consequently, the heterogeneous fault system might be erroneously interpreted as homogeneous. In our tests the limiting angle for reliable separation of stress tensors was found to be 25° (Test 1 (a), results in Table 1 (a)) when large angular noise between theoretical and actual direction of slip along the faults is present in the data. However, with no noise in the data, the limiting angle was much smaller (10° in the Test 1 (b), results in Table 1 (b)).

Acknowledgements

The authors are grateful to Michal Nemcok for his careful review and many constructive comments. We also greatly appreciate the useful comments of an anonymous reviewer and the thorough editorial handling of Bob Holdsworth.

Appendix A. Approximation of the object function in the case of large angular misfits between predicted and actual direction of slip along the faults

The object function can be approximated with an integral:

$$F \approx \frac{K}{\sqrt{2\pi}s_0}\int_{-\pi}^{+\pi}\exp\left(-\left[\frac{(\alpha-\overline{\alpha})^2}{2s_0^2}+\frac{\alpha^2}{2s^2}\right]\right)\mathrm{d}\alpha$$
$$=\frac{K}{\sqrt{2\pi}s_0}\exp\left(-\frac{\overline{\alpha}^2}{2s_0^2}\right)\int_{-\pi}^{+\pi}\exp\left(-\left[\frac{\alpha^2}{2s_0^2}+\frac{\alpha^2}{2s^2}\right]+\frac{\alpha\overline{\alpha}}{s_0^2}\right)\mathrm{d}\alpha = I_1. \quad (A.1)$$

I_1 is the value of the integral. Because $-\pi \leq \alpha \leq \pi$ and $-\pi \leq \overline{\alpha} \leq \pi$, it follows:

$$I_1 \leq \frac{K}{\sqrt{2\pi}s_0}\exp\left(-\frac{\overline{\alpha}^2}{2s_0^2}\right)\int_{-\pi}^{+\pi}\exp\left(-\left[\frac{\alpha^2}{2s_0^2}+\frac{\alpha^2}{2s^2}\right]+\frac{\pi^2}{s_0^2}\right)\mathrm{d}\alpha$$

$$\leq \frac{K}{\sqrt{2\pi}s_0}\exp\left(-\frac{\overline{\alpha}^2}{2s_0^2}+\frac{\pi^2}{s_0^2}\right)\int_{-\infty}^{+\infty}\exp\left(-\left[\frac{\alpha^2}{2s_0^2}+\frac{\alpha^2}{2s^2}\right]\right)\mathrm{d}\alpha$$

$$= \frac{K}{\sqrt{s_0^2/s^2+1}}\exp\left(-\frac{\overline{\alpha}^2}{2s_0^2}+\frac{\pi^2}{s_0^2}\right). \quad (A.2)$$

Therefore:

$$F \leq \frac{K}{\sqrt{s_0^2/s^2+1}}\exp\left(\frac{\pi^2}{s_0^2}\right)\exp\left(-\frac{\overline{\alpha}^2}{2s_0^2}\right). \quad (A.3)$$

References

Angelier, A., Mechler, P., 1977. Sur une méthode graphique de recherche de constraintes principales également utilisable et en séismologie: la méthode des dièdres droits. Bulletin Société Géologique de la France 19, 1309–1318.

Angelier, J., 1979. Determination of the mean principal directions of stress for a given fault population. Tectonophysics 56, T17–T26.

Angelier, J., 1984. Tectonic analysis of fault slip data sets. Journal of Geophysical Research 89, 5835–5848.

Angelier, J., 1989. From orientation to magnitudes in paleostress determinations using fault slip data. Journal of Structural Geology 11, 37–50.

Angelier, J., 1994. Paleostress Determinations. In: Hancock, P.L. (Ed.), Continental Deformations. Pergamon Press, Tarrytown, N.Y., pp. 53–100.

Arlegui-Crespo, L.E., Simón-Gómez, J.L., 1998. Reliability of paleostress analysis from striations in near multidirectional extension stress fields. Example from the Ebro Basin, Spain. Journal of Structural Geology 20, 827–840.

Armijo, R., Carey, E., Cisternas, A., 1982. The inverse problem in microtectonics and the separation of tectonic phases. Tectonophysics 82, 145–160.

Bishop, A.W., 1966. The strength of soils as engineering materials. Geotechnique 16, 91–130.

Bott, M.H.P., 1959. The mechanisms of oblique slip faulting. Geological Magazine 96, 109–117.

Carey, E., Brunier, B., 1974. Analyse théoretique et numérique d'un modèle mécanique élémentaire appliqué a l'étude d'une population de failles. Comptes Rendus de l'Académie des Sciences, Paris D279, 891–894.

Dupin, J.-M., Sassi, W., Angelier, J., 1993. Homogeneous stress hypothesis and actual fault slip: a distinct element analysis. Journal of Structural Geology 15, 1033–1043.

Etchecopar, A., Vasseur, G., Daigniers, M., 1981. An inverse problem in microtectonics for the determination of stress tensors from fault striation analysis. Journal of Structural Geology 3, 51–65.

Fleischman, K.H., Nemcok, M., 1991. Paleostress inversion of fault/slip data using the shear stress solution of Means (1989). Tectonophysics 196, 195–202.

Fry, N., 1992. A robust approach to the calculation of paleostress fields from fault plane data: discussion. Journal of Structural Geology 14, 635–637.

Fry, N., 1999. Striated faults: visual appreciation of their constraint on possible paleostress tensors. Journal of Structural Geology 21, 7–21.

Fry, N., 2001. Stress space: striated faults, deformation twins, and their constraints on paleostress. Journal of Structural Geology 23, 1–9.

Galindo-Zaldivar, J., González-Lodeiro, F., 1988. Faulting phase differentiation by means of computer search on a grid pattern. Annales Tectonicae 2, 90–97.

Hardcastle, K.C., 1989. Possible paleostress tensor configurations derived from fault-slip data in Eastern Vermont and Western New Hampshire. Tectonics 8, 265–284.

Hardcastle, K.C., Hills, L.S., 1991. Brute3 and Select: quickbasic 4 programs for determination of stress tensor configurations and separation of heterogeneous. Computer and Geosciences 17, 23–43.

Huang, Q., 1988. Computer-based method to separate heterogeneous sets of fault-slip data into sub-sets. Journal of Structural Geology 10, 225–237.

Jaeger, J.C., Cook, N.G.W., 1969. Fundamentals of Rock Mechanics. Methuen, London.

Liesa, C.L., Lisle, R.J., 2004. Reliability of methods to separate stress tensors from heterogeneous fault-slip data. Journal of Structural Geology 26, 559–572.

Marrett, R., Peacock, D.C.P., 1999. Strain and stress. Journal of Structural Geology 21, 1057–1063.

Michael, A.J., 1984. Determination of stress from slip data: faults and folds. Journal of Geophysical Research 89, 11517–11526.

Nemcok, M., Kovác, D., Lisle, R.J., 1999. A stress inversion procedure for polyphase calcite twin and fault/slip data sets. Journal of Structural Geology 21, 597–611.

Nemcok, M., Lisle, R.J., 1995. A stress inversion procedure for polyphase fault/slip data sets. Journal of Structural Geology 17, 1445–1453.

Orife, T., Lisle, R.J., 2003. Numerical processing of paleostress results. Journal of Structural Geology 25, 949–957.

Orife, T., Lisle, R.J., 2006. Assessing the statistical significance of paleostress estimates: simulations using random fault-slips. Journal of Structural Geology 28, 952–956.

Otsubo, M., Sato, K., Yamaji, A., 2006. Computerized identification of stress tensors determined from heterogeneous fault-slip data by combining the multiple inverse method and k-means clustering. Journal of Structural Geology 28, 991–997.

Pollard, D.D., Saltzer, D., Rubin, A.M., 1993. Stress inversion methods: are they based on faulty assumptions? Journal of Structural Geology 15, 1045–1054.

Pollard, D.D., 2000. Strain and stress: discussion. Journal of Structural Geology 22, 1359–1367.

Ranalli, G., 2000. Rheology of crust and its role in tectonic reactivation. Journal of Geodynamics 30, 3–15.

Ranalli, G., Yin, Z.-M., 1990. Critical stress difference and orientation of faults in rocks with strength anisotropies: the two-dimensional case. Journal of Structural Geology 12, 1067–1071.

Reches, Z., 1987. Determination of the tectonic stress tensor from slip along the faults that obey the Coulomb yield condition. Tectonics 6, 849–861.

Reches, Z., Baer, G., Hatzor, Y., 1992. Constraints on the strength of the upper crust from stress inversion of fault slip data. Journal of Geophysical Research 97, 12.481–12.493.

Sato, K., Yamaji, A., 2006. Embedding stress difference in parameter space for stress tensor inversion. Journal of Structural Geology 28, 957–971.

Schellart, W.P., 2000. Shear test results for cohesion and friction coefficients for different granular materials: scaling implications for their usage in analogue modelling. Tectonophysics 324, 1–16.

Shan, J., Suen, H., Lin, G., 2003. Separation of polyphase fault/slip data: an objective-function algorithm based on hard division. Journal of Structural Geology 25, 829–840.

Shan, Y., Lin, G., Li, Z., 2004. A stress inversion procedure for automatic recognition of polyphase fault/slip data sets. Journal of Structural Geology 26, 919–925.

Shan, Y., Lin, G., Li, Z., Zhao, C., 2006. Influence of measurement errors on stress estimated from single-phase fault/slip data. Journal of Structural Geology 28, 943–951.

Sibson, R.H., 1985. A note on fault reactivation. Journal of Structural Geology 7, 751–754.

Sibson, R.H., 1989. High-angle reverse faulting in northern New-Brunswick, Canada, and its implications for fluid pressure levels. Journal of Structural Geology 11, 873–877.

Simón-Gómez, J.L., 1986. Analysis of a gradual change in stress regime: example from the eastern Iberian Chain. Tectonophysics 124, 37–53.

Tikoff, B., Wojtal, S.F., 1999. Displacement control of geologic structures. Journal of Structural Geology 21, 959–967.

Twiss, R.J., Unruh, J.R., 1998. Analysis of fault slip inversions: do they constrain stress or strain rate? Journal of Geophysical Research 103, 12,205–12,222.

Wallace, R.E., 1951. Geometry of shearing stress and relation to faulting. Journal of Geology 59, 118–130.

Watterson, J., 1999. The future of failure: stress or strain? Journal of Structural Geology 21, 939–948.

Will, T., Powell, R., 1991. A robust approach to the calculation of paleostress fields from fault plane data. Journal of Structural Geology 13, 813–821.

Yamaji, A., 2000a. Multiple inverse method applied to mesoscale faults in mid Quaternary sediments near the triple trench junction off central Japan. Journal of Structural Geology 22, 429–440.

Yamaji, A., 2000b. The multiple inverse method: a new technique to separate stresses from heterogeneous fault-slip data. Journal of Structural Geology 22, 441–452.

Yamaji, A., 2003. Are the solutions of stress inversion correct? Visualization of their reliability and the separation of stresses from heterogeneous fault-slip data. Journal of Structural Geology 25, 241–252.

Yamaji, A., Otsubo, M., Sato, K., 2006. Paleostress analysis using the Hough transform for separating stresses from heterogeneous fault-slip data. Journal of Structural Geology 28, 980–990.

Yin, Z.-M., Ranalli, G., 1992. Critical stress difference, fault orientation and slip direction in anisotropic rocks under non-Andersonian stress systems. Journal of Structural Geology 14, 237–244.

Yin, Z.-M., Ranalli, G., 1995. Estimation of the frictional strength of faults from inversion of fault-slip data: a new method. Journal of Structural Geology 17, 1327–1335.

Further reading

Angelier, J., 1990. Inversion of field data in fault tectonics to obtain the regional stress – III. A new rapid direct inversion method by analytical means. Geophysical Journal International 103, 363–376.